A USDOT NATIONAL
UNIVERSITY TRANSPORTATION CENTER

Carnegie Mellon University

SMART AND EQUITABLE PARKS: QUANTIFYING RETURNS ON INVESTMENTS BASED ON PROBABILISTIC MOBILITY-DEPENDENT CORRELATES OF PARK USAGE USING CYBER-PHYSICAL SYSTEM TECHNOLOGIES

FINAL RESEARCH REPORT

Katherine A. Flanigan
Department of Civil and Environmental Engineering
Carnegie Mellon University
Pittsburgh, PA 15213
ORCiD: 0000-0002-2454-5713
kaflanig@cmu.edu

Additional Contributors to Acknowledge: Karen Lightman, PhD Student Lindsay Graff, PhD Student Cheyu Lin, Associate Professor Sean Qian

Contract # 69A3551747111

ABSTRACT
Parks are integral to the success of any vibrant city and have long been touted as engines of economic growth that also improve public health, clean the air, manage stormwater, and enable patrons to commune with nature while enjoying a rich set of social experiences within their community. Today, 165 parks are maintained in Pittsburgh ranging from small neighborhood parks to large greenways. Unfortunately, the financial constraints of the city have challenged its ability to maintain its parks; Pittsburgh parks are underinvested in comparison to both regional and aspirational peers. A key challenge for local governments is to develop and maintain parks and other public goods in ways that equitably distribute benefits to health, well-being, livability, accessibility to essential services, and the economy. This is critical because in areas where essential services are unevenly distributed across a community, parks and greenways often lead to a bifurcation: they either serve as barriers that result in social polarization, or serve as enabling public facilities that connect citizens in under-resourced areas to their wider communities and services; the polarizing or unifying nature of parks is heavily dependent on the configuration and health of surrounding mobility services. The overarching goal of this work is to explore urban park use and correlates of use (measured by time-dependent accessibility) in order to bring to light ways in which city officials and planners can quantify data-driven returns on potential investments to parks and mobility services and implement changes that will more equitably distribute these benefits.

Keywords: accessibility, emerging mobility, micromobility, mobility service, parks, reliability

INTRODUCTION

Parks are integral to the success of any vibrant city and have long been touted as engines of economic growth that also improve public health, clean the air, manage stormwater, and enable patrons to commune with nature while enjoying a rich set of social experiences within their community (*1, 2*). High-quality park systems attract employers, accelerate the pace of commercial development, and generate new tax revenue.

Pittsburgh has experienced a severe decline in population and economic opportunity over the past 60 years largely due to the decline and relocation of industrial manufacturing. Pittsburgh's prosperity during the early-to-mid 20th century allowed the city to invest extensively in parks leaving a legacy that benefits the community today. By the late 1960's, however, the economy began to contract resulting in population decline (0.67 million in 1950 to 0.30 million in 2019). Erosion of the city tax base also led to decades of underinvestment in infrastructure, including park facilities. Today, 165 parks are maintained in Pittsburgh ranging from small neighborhood parks to large greenways. Evidence of the distribution of parks is that approximately 92% of Pittsburgh residents live within a half-mile walk of a park (*3*). Despite having better access to open space than their regional peers, Pittsburgh parks are underinvested in comparison to peers (*3*). The dwindling resources available for maintenance and upkeep, coupled with aged park and recreation facilities, have resulted in deteriorating conditions. Despite efforts by the City's Department of Public Works to do more with less, today more than half of all parks in Pittsburgh are in fair or poor condition; more than 95% of 3,400 Pittsburgh residents interviewed believe the parks need more resources (*4*). In 2019, Pittsburgh residents passed a Parks Tax referendum that amended the City of Pittsburgh Home Rule Charter to establish a trust fund for improving Pittsburgh parks.

To help inform the allocation of the Park Tax funds (approximately $10 million/year), the Pittsburgh Parks Conservancy (PPC) developed the Restoring Parks Plan (*5*), which is a publicly supported and transparent equitable investment strategy encompassing all park and recreation sites within Pittsburgh. The aim of the Restoring Parks Plan is to upgrade and modernize parks and recreation facilities and programs throughout Pittsburgh by investing in four key budget areas: maintenance, rehabilitation, capital projects, and programming. In achieving these goals, the PPC is committed to transparency (i.e., clear and open budgeting), spending equitably across the city (i.e., prioritizing the parks and communities that need it most), and citizen input and guidance (i.e., public accountability to ensure goals are accomplished). To meet these commitments, the PPC developed a Park Scoring Database (*6*) that comprises the first-ever comprehensive inventory of all park and recreation sites, assessment information on park needs, community needs, and public priorities, as well as extensive demographic, health, community condition, and ecological information. Community input was collected over the course of 240 listening tours that were conducted across 70 Pittsburgh neighborhoods. In addition to feedback collected during the tours, 3,400 surveys were administered to determine public priorities for park investment. Leveraging the Park Scoring Database, the PPC aims to evaluate allocation scenarios and map out investment strategies for the City's parks, which will provide a quantifiable backdrop for the myriad of vital qualifiers for improving public health, access, and community investment, all of which are "people centric." Despite the wealth of community research tools and information provided by the Restoring Parks Plan, the PPC has struggled to make targeted investments because they are unable to quantify the performance and accessibility of park facilities. Thus, a key aim is to 1) quantitatively measure and integrate the performance of parks into the Park Scoring Database, and 2) develop and maintain parks in ways that equitably distribute benefits. In this sense, they seek to make decisions based

on the ability of populations to *both* access and benefit sufficiently from park resources.

The historical public facility management paradigm ignores the value of parks and casts it as a problem of achieving equity based on static spatial distribution metrics. Existing planning and maintenance decisions aim to evenly distribute parks among populations spatially with little to no consideration of the location or measurable quality of mobility services that link populations to parks (*7–13*). There is, however, a silver lining when the narrative is shifted to a more dynamic view of accessibility from a transportation perspective. The proliferation of shared transportation modes and micromobility infrastructure has changed the way that people travel within urban areas. People are no longer constrained to riding their personal vehicle or using the fixed-schedule public transit network to reach their final destination. Rather, they may use emerging mobility options to construct convenient trips from end-to-end. By harnessing the full extent of the multimodal network, people can access a larger set of essential resource destinations, such as parks (other examples include grocery stores, work places, hospitals etc.).

The overarching aim of this work is to 1) integrate privacy-preserving cyber-physical system technologies that measure park usage into Pittsburgh parks (i.e., quantitatively measure and integrate the performance of parks into the Park Scoring Database), 2) develop a novel multimodal network modeling framework that accounts for five major factors across all travel modes: day-to-day average travel time, price, reliability represented by day-to-day travel time variability, safety risks, and discomfort (i.e., quantify community accessibility to parks across time and space), and 3) quantify the total system performance through a probabilistic spatio-temporal network reliability analysis in which the failure limit state is defined as any subset of a community's population not being able to access and/or benefit sufficiently from its surrounding parks. Note that this is a function of both park performance and accessibility. For the purpose of making optimal urban planning and investment decisions, through this framework we will be able to simulate the effects of specific park and mobility service maintenance, rehabilitation, and capital projects on the probabilistic health and weights of network nodes and linkages, as well as the connectivity of the network. In other words, this framework enables decision makers to understand which mobility options have the potential to improve accessibility, gain insights into spatio-temporal mobility disparities across different populations with different needs, and incorporate real-time metrics into their Park Score database to assess the need for asset improvements.

This report is structured as follows. First, a novel multimodal network modeling framework is presented. The design of the multimodal network, assignment of travel costs, and the process for measuring accessibility between an O-D pair is presented. The proposed method is demonstrated using a subset of the transportation network in Pittsburgh, PA, and the results of the study are discussed. Second, a framework for the probabilistic assessment of how well subpopulations access (as defined in the subsequent section) and benefit from the parks in and around their communities is presented. Third, the development of a privacy-preserving sensing architecture used to measure the usability of walkable/bikable paths in parks is presented. The report concludes with an overview of the findings, conclusions, and recommendations.

SECTION 1: MEASURING TIME-DEPENDENT ACCESSIBILITY WITH EMERGING MOBILITY OPTIONS

The proliferation of shared transportation modes and micromobility infrastructure has changed the way that people travel within urban areas. People are no longer constrained to riding their personal vehicle or using the fixed-schedule public transit network to reach their final destination.

Rather, they may use emerging mobility options to construct convenient trips from end-to-end. By harnessing the full extent of the multimodal network, people can access a larger set of essential resource destinations, such as parks (other examples include grocery stores, work places, hospitals etc.).

As the mobility landscape evolves, several cities including Austin, Boston, and Portland have developed plans to make their multimodal transportation networks more efficient, affordable, reliable, safe, and equitable, all with the goal of improving accessibility to locations that provide goods and services (*14–16*). Ensuring successful implementation requires a way for the cities to measure the ability of different communities to access these points of interest. To address this measurement challenge, the first part of this project develops a multimodal network modeling framework that quantifies time-dependent accessibility in a transportation network. The mobility options included are personal vehicle, transportation network companies (TNC), car share, public transit, personal bike, bike share, scooter, and walk. Planners can use the framework to compare the accessibility of different origin-destination (O-D) pairs (in this project, the origins are sub-populations, or users, and the destinations are park facilities) across time and space and evaluate where, when, and why mobility is underserved. The proposed method can also be used to determine how changes to the network, such as the addition of micromobility services or a decrease in public transit fare, affect accessibility of points of interest for different neighborhoods. While this framework is used to understand how populations access park facilities in this work, this powerful framework can also be used more generally to understand a wide range of O-D pairs with essential service destinations such as grocery stores, work places, hospitals etc.

For this first part of the project, the research goal is related to the objective of the literature in Table 1, which also seeks to measure point-of-interest accessibility for the purpose of planning. However, the analysis in these papers neglects three factors that impact an assessment of accessibility: multimodal travel, a more comprehensive travel cost function, and time-dependency. This research aims to fill that gap by including all relevant transportation options, accounting for multiple travel cost factors, and incorporating travel costs that vary by departure time.

In these papers and others (*24*), accessibility is quantified in different ways. Frequently used accessibility metrics are contour measures, which count the number of "opportunities" (i.e. points of interest) within some travel time contour relative to an origin, and gravity measures, which calculate the sum of opportunities discounted by their travel time relative to an origin. Of note is the fact that these accessibility metrics, among others, require a determination of the shortest path by travel time between O-D pairs. Consequently, this paper chooses to measure accessibility as the cost of the shortest path between an O-D, where cost is defined with respect to travel time, price, reliability, safety, and discomfort.

This work thereby bridges the aforementioned literature on accessibility analysis with the body of research concerned with least-cost multimodal route-finding in large-scale networks. Much of the previous multimodal route-finding research, summarized in Table 2, is focused on the process of efficiently finding optimal paths with respect to the commonly used criteria of travel time and number of transfers. This process-driven research, which mostly centers on improving algorithmic efficiency, is necessary for the development of mobile applications such as Moovit and Citymapper that people use for real-time navigation in an increasingly multimodal world (*25*). Unlike this type of routing research, this work does not concentrate on the algorithmic or runtime efficiency components of pathfinding, nor does it outline a data-gathering procedure for finding a multimodal route in real-time. Instead, the research objective is to design a comprehensive multi-

TABLE 1: Literature Review: Accessibility Evaluation

Study	Objective	Population Considered	Accessibility Metric(s)	Travel Modes	Travel Cost	Time-dependent Analysis
Tribby and Zandbergen (*17*)	measure and compare accessibility by way of PT	–	TT of SP	PT, walk	TT	✓
Djurhuus et al. (*18*)	determine individual-based accessibility areas by way of PT	–	total accessible area	PT, walk, personal bike	TT	✓
El-Geneidy et al. (*19*)	measure and compare accessibility by way of PT	socially disadvantaged	cumulative opportunities	PT, walk	TT, price	✓
Chen et al. (*20*)	measure and compare accessibility by way of PT	–	1. gravity metric 2. TT of SP, weighted by destination importance	PT, walk	TT	–
Järv et al. (*21*)	measure and compare accessibility to services by time of day	–	TT of SP	PT, walk	TT	✓
Carpentieri et al. (*22*)	measure accessibility of elderly people to healthcare services	elderly	gravity metric	PT, walk	TT	–
Yu et al. (*23*)	evaluate multimodal accessibility with resepct to TT and price budgets and under TT uncertainty	–	cumulative opportunities	TNC, PT, walk	TT, price, reliability	–
This paper	measure and compare accessibility between heterogeneous regions in a time-dependent multimodal network	Population characterized by time, location and socio-demo	total cost of SP	personal vehicle, TNC, car share, PT, personal bike, bike share, scooter, walk	TT, price, reliability, risk, discomfort	✓

Notes: "TNC" = transportation network company; "PT" = public transit; "TT" = travel time; "SP" = shortest path; "✓" indicates that time-dependent analysis is possible with the proposed method; "–" indicates that time-dependent analysis is not possible

TABLE 2: Literature Review: Multimodal Route-finding

Study	Use Case	Travel Cost	Included Travel Modes		Case Study	
			Shared Micromobility	On-demand Service	Network Size	Data Type
Delling et al. (*26*)	RTRP	TT	–	–	>1 million nodes	real
Zhang et al. (*27*)	RTRP	TT + price + effort + discomfort	–	–	>10,000 nodes	real
Delling et al. (*28*)	RTRP	TT, price, inconvenience	✓	✓	>250,000 nodes	real
Hrnčíř and Jakob (*29*)	RTRP	TT	✓	✓	>100,000 nodes	real
Dibbelt et al. (*30*)	RTRP	TT	–	–	>1 million nodes	real
Georgakis et al. (*31*)	RTRP	TT	✓	✓	N/A	N/A
Huang et al. (*32*)	RTRP	TT	–	✓	>6,500 nodes	real
This paper	accessibility analysis	TT + price + reliability + risk + discomfort	✓	✓	>7,500 nodes	real

Notes:
"RTRP" = real time route planning; "TT" = travel time; shared micromobility" includes bike share and scooter; "on-demand service" includes TNC and demand-responsive transit; "generalized travel cost" is a travel impedance that includes additional elements beyond just travel TT; "✓" indicates inclusion by the study; "–" indicates not included by the study; "Network Size" does not include time event nodes from the time-expanded public transit network model

modal network including all possible mobility options for the purpose of examining possible path choices for individual travelers. With this network model, transportation planners can quantify the accessibility of relevant points of interest for different communities to gain insight into where network improvements can be made. This research uses elements of the literature of Table 2 in designing a connected multimodal network model that permits a determination of the shortest path between points.

The rest of this section is structured as follows. First, the design of the multimodal network, assignment of travel costs, and process for measuring accessibility between an O-D pair is presented. Second, the proposed method is demonstrated using a subset of the transportation network in Pittsburgh, PA, and the results of the study are discussed. The final section highlights key conclusions and identifies opportunities for future work.

METHODOLOGY

The process of measuring accessibility in a regional multimodal network involves three stages: designing the multimodal network, defining an edge cost function, and finding the least-cost path

TABLE 3: List of Notation

G_m	graph associated with travel mode m
N_m	set of graph nodes associated with G_m
A_m	set of graph edges associated with G_m
N_{dr}	set of road intersection nodes in the driving network
A_{dr}	set of road segment edges in the driving network
N_{pk}	set of parking nodes
$A_{pk,cnx}$	set of edges that connect parking nodes to their nearest neighbor node in the driving network
N_b	set of road intersection nodes in the bikeable network
A_b	set of road segment edges in the bikeable network
N_{ps}	set of public transit physical stop nodes
N_{rt}	set of public transit virtual route nodes
A_{board}	set of edges from physical stop nodes to associated virtual route nodes, which represent the process of waiting and boarding
A_{alight}	set of edges from virtual route nodes to associated physical stop nodes, which represent the process of alighting
A_{rt}	set of edges between virtual route nodes
N_{bsd}	set of bike share depot nodes
$A_{bsd,cnx}$	set of edges that connect bike share depot nodes to their nearest neighbor node in the bikeable network
A_{bsd}	set of precomputed edges that connect bike share depot nodes
N_{csd}	set of car share depot nodes
$A_{csd,cnx}$	set of edges that connect car share depot nodes to their nearest neighbor node in the driving network
A_{tx}	set of transfer edges
N_{OD}	set of origin nodes and destination nodes
$A_{OD,cnx}$	set of edges that connect the origin and destination nodes to the component networks

between selected O-D pairs based on characteristics of travelers. The first step to constructing the multimodal network is to model each single-mode transportation network as a graph consisting of road intersection nodes and road edges. These graphs are then connected to each other by transfer edges at relevant nodes where transfers are likely to take place, which results in a single multimodal graph, or "supernetwork" (*33, 34*). Once the network topology is determined, a time-varying travel cost is assigned to each edge. In this work, the travel cost is given by the weighted sum of travel time, price, reliability, and risk. A time-dependent shortest path algorithm is subsequently used to find the least-cost path between selected O-D pairs for different departure times. Table 3 specifies the notation used in this report.

Multimodal Network Design

This work considers an exhaustive list of possible travel modes: personal vehicle (PV), transportation network company (TNC), car share (CS), public transit (PT), personal bike (PB), bike share (BS), scooter (S), and walking (W). The component network for each travel mode m is modeled

separately and represented by a graph $G_m = (N_m, A_m)$. Whereas some modes (e.g., TNCs) allow travelers to hail a ride or exit at any point in that mode's network, others such as public transit and bike share require that commuters only move between fixed points. The supernetwork consists of these component networks joined together by transfer edges. Origin and destination nodes are joined to certain points in the component networks by connector edges. It is important to note that this network only models outbound trips where a person commutes from their neighborhood to a point of interest. This distinction is necessary because modeling the inbound trip would require the reversal of some transfer edges and connection edges within the personal vehicle and car share component networks.

Personal Vehicle

The personal vehicle network $G_{PV} = (N_{dr}, N_{pk}, A_{dr}, A_{pk,cnx})$ consists of the typical street map used by drivers. Road intersections comprise the graph's core set of intersection nodes, which are connected by road segment edges. A parking connector edge joins each parking node to its nearest nearest neighbor street intersection node in the driving network. The directional connector edge goes from the street intersection node to the parking node since this network model only considers the outbound trip; once a person parks their car, they do not use their personal vehicle again on the outbound trip.

TNCs

The TNC network $G_{TNC} = (N_{dr}, A_{dr})$ is created by duplicating the personal vehicle network and removing parking nodes and their connector edges. Riders in the TNC network can choose their point of entry and exit at their convenience.

Car Share

Commuters using a car share rental vehicle, which they must pick up at a depot, use the personal vehicle network to drive and park their shared vehicle. The car share component network can be thus modeled as $G_{CS} = (N_{dr}, N_{pk}, N_{csd}, A_{dr}, A_{pk,cnx}, N_{csd,cnx}, A_{csd,cnx})$. In this model, N_{csd} specifies the set of all car share depot locations and $A_{csd,cnx}$ denotes the set of connector edges that join the each depot to its nearest neighbor node in the rest of the network. Modeling only the outbound trip requires that these directional edges go from the depot to the street intersection node; after a commuter rents a vehicle, they do not return the vehicle on the same outbound trip (the vehicle is returned on the inbound trip).

Public Transit

A time-dependent network $G_{PT} = (N_{ps}, N_{rt}, A_{board}, A_{alight}, A_{rt})$ is used to model the public transit network (*35*). This model contains two types of nodes: physical stop nodes N_{ps} and route nodes N_{rt}. Physical stop nodes represent actual locations in the network where travelers board or alight a bus. Since more than one bus route can pass through a physical stop, each stop is also linked to one or more route nodes. The edge from a stop node to a route node represents the cost of waiting and boarding, whereas the edge from a route node to a stop node represents the cost of alighting. Hence, it is possible to switch routes at one physical stop by using an alighting edge tied to one route node and a boarding edge tied to a different route node. The graph also consists of route traversal edges in the set A_{rt} which connect route nodes, where the weight of each route edge corresponds to the cost of traveling along that particular bus segment. The time-dependent

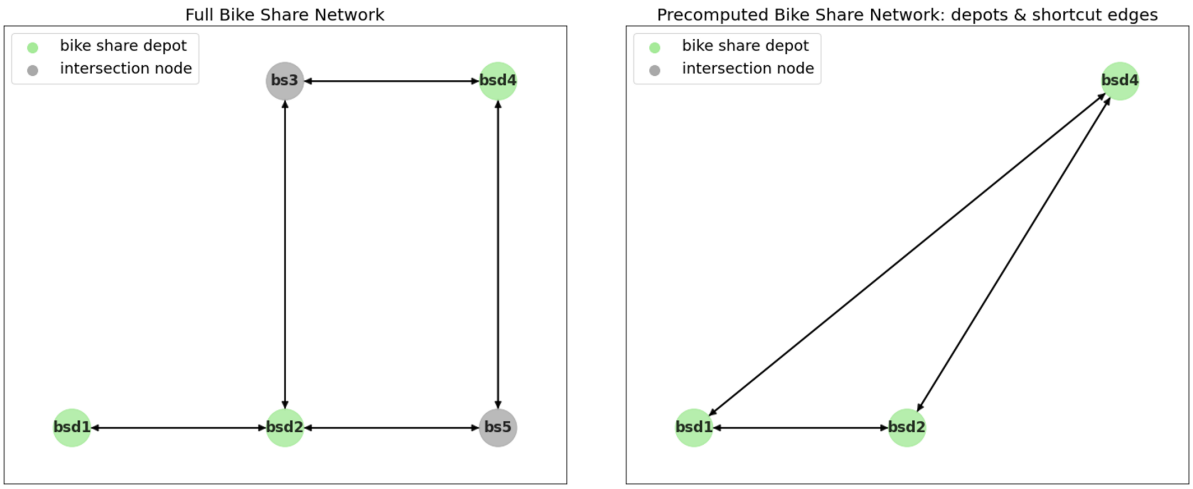

FIGURE 1: An example showing how precomputing shortcut bike share edges can reduce the size of the network.

model of public transit was selected over the time-expanded model for its smaller size and easier integration with other component graphs.

Personal Bike

The personal bike network $G_{PB} = (N_b, A_b)$ includes road edges that are considered bikeable according to the OSMnx package in Python (*36*). Per the OSMnx package definition, a road is considered bikeable unless it is a highway, private road, or a street specifically marked for pedestrians.

Bike Share

The original bike share network $G_{BS} = (N_b, N_{bsd}, A_b, A_{bsd_cnx})$ is formed by duplicating the personal bike network and then adding bike share depot nodes and bike share connector edges. The depot nodes represent the locations where travelers can pick up or drop off a shared bicycle. A bidirectional bike share connector edge joins each depot node to its nearest neighbor intersection node in the bike share network, similar to how parking and car share depot connector edges are implemented.

Since a traveler using a shared bike must pick up and drop off the bicycle at a depot, it is possible to consolidate the bike share network into a set of depot nodes and depot edges. Shortcut bidirectional depot edges connect depot nodes directly to each other, where a shortcut edge between nodes represents the least-cost path between them. The precomputed network $G_{BS,pre} = (N_{bsd}, A_{bsd})$ is useful for simplifying the graph and expediting processing time when evaluating shortest paths in the full multimodal network.

Scooter

The scooter network $G_S = (N_b, A_b)$ is modeled as a duplicate of the personal bike network. The inherent assumption is that scooters may use the same roads as a bicycles. Explicitly modeling the location of a scooter pickup node is not possible since riders may leave scooters in any valid parking spot in the network. Given that this network model is being used for planning purposes as opposed to real-time navigation, it is also not necessary to identify exact scooter locations. Instead,

data can be used to estimate the average distance that a person must walk in order to pick up the nearest scooter. This estimation process, which is embedded in the procedure for building transfer edges, is explained in section 4.1.9

Walk
The full walking network is not explicitly modeled in this design. Rather, only certain relevant walking segments are included. The relevant walking segments pertain to the following scenarios: transfers between two component networks, connections from the origin to the component networks, and connections from the component networks to the destination. For example, a transfer between a bike share depot and a public transit physical stop is modeled as a single walking segment whose approximate distance is equivalent to the Haversine distance between the depot and stop node. This modeling decision removes the need to include the full walking network, which simplifies the design.

Transfer Edges
After modeling each component network, transfer edges are created to connect component networks to each other. Transfer edges that form the set A_{tx} are directional and assumed to be traversed by walking. Locations in a component network where a mode change may take place are called switch points, following the approach of (*37*). If the switch point is at a predetermined location (e.g bus stop, bike share depot, parking node), it is denoted a "fixed pickup" or "fixed drop-off" node; if the switch point changes depending on the commuter's needs (e.g., TNC pickup point), it is considered a "flexible pickup" or "flexible drop-off" node. Each transfer link is constructed by joining a switch point in one component network to a switch point in another. A multimodal graph with transfer edges is depicted in Figure 2, which demonstrates a small example network that includes the bike share, public transit, and TNC modes. The component networks in this figure are slightly offset for visualization purposes, since they physically overlap.

Building transfers efficiently requires the specification of constraints on allowable switches between travel modes. Figure 3 enumerates the plausible mode changes, where the arrows indicate the direction of the change. This list of allowable changes between modes is based on practical considerations. One such assumption is that travelers using a personal or car share vehicle can switch from the driving mode to another mode only after dropping their vehicle in a parking zone. In addition, changing modes from personal bike to public transit is enabled by the presence of a bike rack on a bus. It is also assumed that intermediate bike parking is not available and bike racks do not exist on other vehicles, which implies that travelers who ride their personal bike on any part of a path can use only a combination of the personal bike, public transit, and walking networks. In addition, any modal transfer can be associated with a specific generalized cost that influence the optimal path finding, e.g., convenience, cost, fare discount or discomfort. This is achieved by imposing node-based generalized cost to associate any specific edge-to-edge movement. The cost can be set arbitrarily small to imply seamless connection, negative to imply fare discount offered to use two specific modes sequentially, or arbitrarily large to imply prohibition between any two modes.

An additional assumption in this network design is that travelers are willing to walk a distance less than or equal to W when transferring modes. The implication is that for every fixed drop-off node in any component network, there exists a "walking catchment zone" (WCZ) which contains all surrounding nodes within a Haversine distance of W. Though this approximation

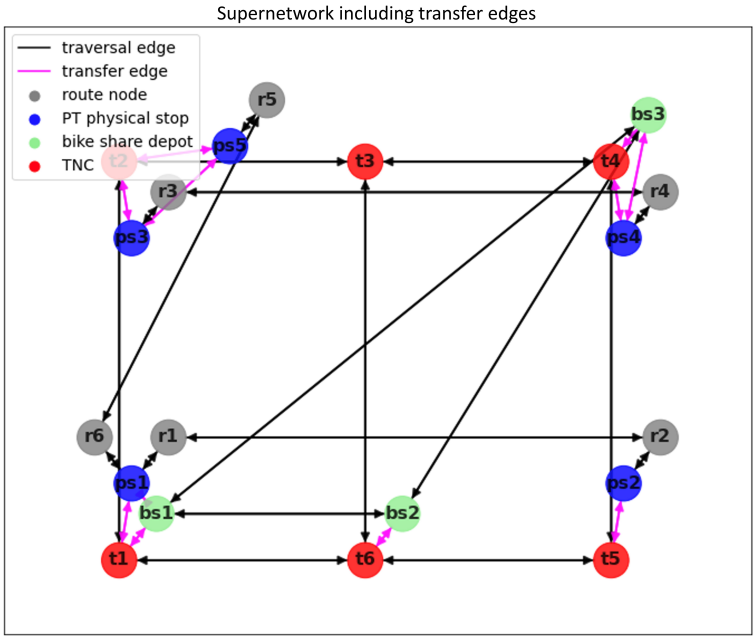

FIGURE 2: Example supernetwork with transfer edges for bike share, public transit, and TNC networks.

underestimates true network walking distance, it is assumed to closely represent actual distance due to the presence of walking shortcuts. However, it is not necessary to build a WCZ for flexible pickup/drop-off networks. The reason is that, when given a choice of where to be dropped off in a flexible network, travelers would logically always choose the drop-off node is that nearest the next pickup node they wish to use. Thus, if the transfer is allowed, a transfer edge is drawn from a fixed drop-off node to the nearest node in flexible pickup network and vice versa for a fixed pickup node.

In previous research (*26, 27*), transfer edges are created by joining switch points in one component graph to their nearest neighbor in the reference walking network. Constraints relating to the mode sequence are then enforced at runtime by the use of a specific label-constrained algorithm or by the inclusion of a only a subset of component graphs. The approach in this report, which is similar to (*37*), is different in the sense that transfer links embed mode sequence constraints. This eliminates the need to use a label constrained shortest path algorithm.

Origin and Destination Connectors

Transportation planning analysis is typically conducted on an aggregated geographic level, where the geographic entity is selected to represent the travel patterns of many people within the entity (*38*). Common geographic units include traffic analysis zones and census block groups. The proposed network model uses the centroids of the geographic unit as both origins and destinations so that accessibility between regions can be measured. The set of origin and destination nodes is called by N_{OD}. Each origin is connected to nearby pickup nodes by origin connector edges and each drop-off node is connected to nearby drop-off nodes by destination connector edges. An O-D pair and its associated connector edges, denoted by $A_{OD,cnx}$, is added to the network on the fly at the time of evaluation to minimize network size.

Mode 1		Mode 2
Public Transit	⟷	Public Transit
Public Transit	⟷	Bike Share
Public Transit	⟷	TNC
Public Transit	⟷	Personal Bike
Public Transit	⟷	Scooter
Public Transit	→	Car Share
TNC	⟷	Bike Share
TNC	→	Car Share
Personal Vehicle	→	Public Transit
Personal Vehicle	→	TNC
Personal Vehicle	→	Bike Share
Personal Vehicle	→	Scooter
Bike Share	⟷	Scooter
Bike Share	→	Car Share
Scooter	→	Car Share
Walk	⟷	*Any Mode*

FIGURE 3: Allowable mode changes.

The procedure to build O-D connector edges is similar to the process of creating transfer edges. The idea is that a traveler can transfer from the origin to any component graph that has a fixed pickup node within the origin's WCZ, and vice versa for fixed drop-off nodes within a destination's WCZ. However, if there is no fixed pickup node within an origin's WCZ for a specific mode, an edge is instead created from the origin to the nearest fixed pickup node in the mode's component network. This modeling choice reflects the reality of a commuter's decision-making process, as they are they are more likely to walk a longer distance on the first leg of their journey rather than at an intermediate stage. The same exception is made if all fixed drop-off nodes of a specific mode type exist outside a destination's WCZ. An origin connector edge also joins the origin to its nearest neighbor in flexible pickup networks, and a destination connector edges joins the destination to its nearest neighbor in flexible drop-off networks.

Supernetwork

The multimodal graph is defined as the union of all component networks, transfer edges, O-D nodes, and O-D connector edges:

$$G_{MM} = G_{PV} \bigcup G_{TNC} \bigcup G_{CS} \bigcup G_{PT} \bigcup G_{PB} \bigcup G_{BS} \bigcup G_{S} \bigcup A_{tx} \bigcup N_{OD} \bigcup A_{OD,cnx} \quad (1)$$

Cost Assignment

Transportation planners can use this network model to measure accessibility between points by departure time. This report defines accessibility from an origin to a destination as the total cost of the least-cost path between them in a multimodal network. Finding the least-cost path requires a cost determination for each edge and node in the graph, followed by the process of running a shortest path algorithm.

Generalized Cost Function

One way that the proposed method distinguishes itself from previous research is by defining the edge cost function as a combination of five time-dependent factors: price, average travel time, reliability, risk, and discomfort. The total cost C of an edge e is defined as a linear combination of the five individual attributes as a function of departure time t, given by equation 2.

$$C_e(t) = \beta_p \cdot p_e(t) + \beta_{TT} \cdot TT_e(t) + \beta_r \cdot r_e(t) + \beta_k \cdot k_e(t) + \beta_D \cdot D_e(t) \tag{2}$$

where p is the price, TT is the average travel time, r is the reliability, k is the risk, and D is the perceived discomfort value. All cost factors are defined with respect to edge e and departure time t. Reliability is measured by the edge's 95$^{\text{th}}$ percentile travel time, following common practice in the transportation engineering field (*39*). The edge's risk k_e is quantified by its unitless risk index x_e multiplied by its average travel time TT_e, where the risk index considers the road segment's vehicle crash rate for vehicle networks or the road segment's availability of micromobility infrastructure for micromobility networks. The discomfort attribute of an edge represents the level of physical exertion required for its traversal. This model assumes that an edge's discomfort attribute is zero for all inactive commuting modes, which includes all modes that use vehicle travel. Active modes, which include biking, walking, and scooter-riding according to the Department the Energy's Alternative Fuels Data Center (*40*), are associated with some degree of physical difficulty. In this work, the discomfort value of an edge D_e is quantified by a discomfort weight parameter d multiplied by the edge's average travel time TT_e. The benefit of defining reliability, risk, and discomfort in terms of travel time is that the attributes are on the same scale such that no single factor completely dominates the cost function.

The β parameters can be interpreted as the dollar value that a person assigns to a single unit of the cost factor. The parameter β_p thus takes on the unitless value of 1, while β_p has units of dollars per minute and is representative of a person's value of time. When conducting analysis, the β parameters can be adjusted based on the population group under consideration or the goals of the transportation planner. For example, a planner interested in bike safety may choose to give higher weight to β_k. A planner may also choose to assign a higher value of time β_{TT} when evaluating path options during commuting hours vs. off-peak hours.

Regarding time dependency, inactive modes are assumed to be unaffected by traffic flow such that all associated edge costs are constant with time. The travel time and reliability of the traversal edges of the personal vehicle, TNC, and car share modes vary with time in accordance with traffic flow, while price is constant. For TNC and car share edges, however, price also changes with time because their price is correlated with usage time. The travel time and reliability of public transit edges are time-dependent as a result of both the fixed schedule and traffic conditions. The risk index and discomfort weight associated with an edge are assumed to remain constant regardless of departure time.

Transfer Edge Costs

The cost vector of a transfer edge consists of the cost attributes that are associated with the shortest walking path between the two nodes that define the edge, in addition to a dollar-valued inconvenience cost that is associated with the act of transferring. The distance of the shortest path can be estimated as the Haversine distance between the two nodes, an approximation that simplifies the transfer edge cost calculation. The price attribute of a transfer edge is considered to be \$0, which

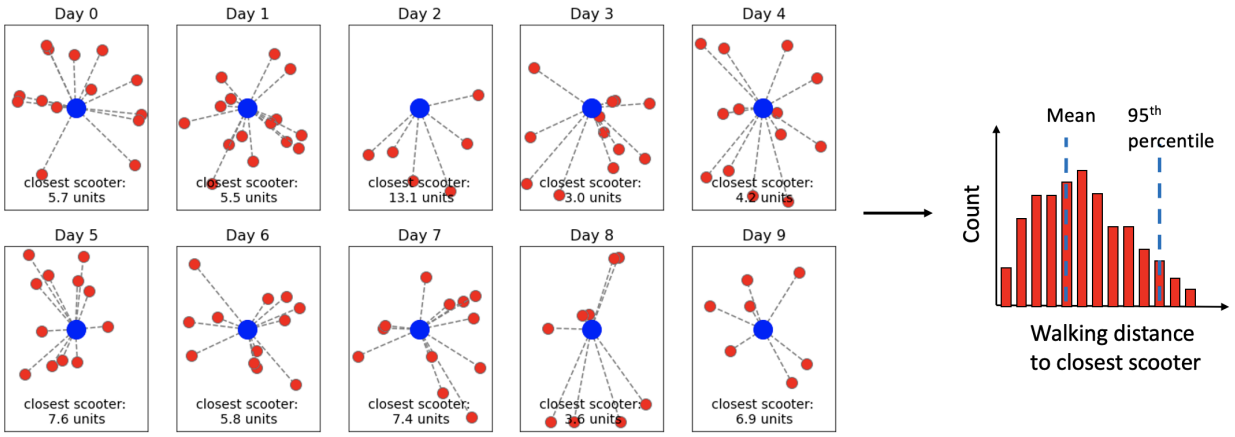

FIGURE 4: An example of 10 historical daily scooter observations (red) for a given time interval shown relative to a specified fixed node (blue). The average and 95th percentile distance to the nearest scooter are used to assign scooter transfer edge costs.

is consistent with the price associated with a walking path, unless parking or other fixed costs are embedded into the edge.

For directional transfer edges that connect fixed drop-off nodes to the nearest intersection node in the flexible scooter network, the time-dependent cost vector is estimated based on historical observations of physical scooter locations. If given the actual location data of all scooters by date and departure time, one can find the distance between any fixed drop-off node and its nearest physical scooter for the specified date and departure time pair. Repeating this process for n days results in a distribution of the distance, which can be converted to walking travel time, from each fixed node to its nearest scooter. From this distribution, the average and 95th percentile walking time from a fixed node to its nearest scooter can be derived. This procedure, which is depicted with an example in Figure 4, can also be used to model the average and 95th percentile waiting time for a TNC vehicle.

Node Costs

In addition to edge costs, movement-based node costs are added to the model. These node costs represent a penalty on moving from one link to another via a particular node. For this network model, movement-based node costs can be used to prevent or discourage certain behavior, such as the usage of two consecutive transfer edges. Without node costs, the least-cost route may consist of several connected transfer edges that effectively create a longer transfer edge whose length exceeds the parameter W defined in the Transfer Edges section. This situation could arise if β_{TT} is low. Since transfer edges are traversed by walking, they have a price of zero and minimal risk and discomfort costs; hence they are desirable from a cost standpoint if value of time is low.

Accessibility Analysis

Once costs are assigned to the multimodal network, it can be used to evaluate accessibility on an O-D level in addition to an origin level or a destination level. On the O-D level, accessibility is defined as the cost of the least-cost path between two points. This use-case will be explored in the

next section. This framework also enables an assessment of origin-level accessibility, where the quantity of essential service destinations reachable by a given origin within some cost threshold can be compared. Destination-based accessibility can be evaluated in a similar manner; policymakers can determine the number of origins able to reach a particular destination to better understand its value to the network. The time-dependent least-cost path necessary for this analysis can be found with the decreasing order of time algorithm presented in (*41*).

CASE STUDY

The proposed methodology is demonstrated on a group of demographically-different neighborhoods in Pittsburgh, PA. In all test cases, the personal vehicle network is excluded from the supernetwork since the population of interest is assumed to not have access to private vehicles. The final supernetwork, inclusive of all traversal, transfer, and O-D connector edges, has 7,924 nodes and 53,988 edges. To test the multimodal route-finding capability, census block group centroids are used as origin and destination nodes. A two-hour departure window divided into thirteen time intervals is considered, and the time-dependent algorithm is provided by open-source code on Github[1] detailed in (*42*).

Network Settings and Data

The area's driving and biking networks are extracted from the Python package OSMnx, which downloads geospatial data from OpenStreetMap and then simplifies the network topology (*36*). Locations of bike share depots, bike lanes, parking meters, and parking rates are obtained from the Western Pennsylvania Regional Data Center (*43*). For simplicity, the parking nodes are consolidated into one representative node per parking zone, represented by the average location of a parking meter within a zone. The cost of parking is calculated as the product of the hourly parking rate and the number of parking hours, which is assumed to be eight hours in accordance with a full work day. Public transit stop locations and route information are provided by the General Transit Feed Specification (GTFS), and the locations of Zipcar (*44*) depots are found by querying Google My Maps (*45*) and downloading the coordinate pairs returned. While this method for extracting car share locations is not entirely accurate, it serves the purpose for testing the model. In the Pittsburgh region, Zipcar runs the car sharing service, POGOH (*46*) operates the bike share system, Spin (*47*) manages the scooter fleet, and Pittsburgh Regional Transit (*48*) acts as the public transit agency.

Assigning cost attributes to the edges requires the specification of several parameters, which are listed in Table 4. Prices for a Zipcar car share, POGOH bike share, Spin scooter, and Port Authority bus ride are obtained from various company or agency websites. Travel speed parameters for bicycles, personal vehicle operating costs, TNC prices, and waiting time for TNC vehicles are based on previous research (*49–53*), with presumed equivalence between scooter and bike speeds. The traversal time between bus stops and average headway between bus trips are both based on GTFS schedule data, and the average waiting for a bus, regardless of the commuter's arrival time at the stop, is assumed to be half of the bus headway time per convention (*54*). To calculate the risk index, the factors considered for the micromobility networks are road type and bike lane presence, while the single factor considered for the driving networks is vehicle crash rate. Movement-based node costs are also added to prevent a route that uses two consecutive transfer edges. Finally, the walking catchment zone parameter W is set at 0.5 miles to prevent transfer or

[1] https://github.com/psychogeekir/MAC-POSTS

O-D connection edge lengths greater than this value.

Data that was not available for this case study is estimated. The unavailable information includes actual historical travel time data for any of the vehicle networks, as well as historical scooter observations. For average traversal time between transit stops, GTFS schedule data is used instead. The average travel time for edges in the driving networks is assumed to be the product of its speed limit, length, and a travel multiplier used to represent the ebb and flow of morning traffic. This multiplier function is generated as a bell-shaped curve with a value of 1 at the start and end of the departure window and a value of 1.5 in the middle of the window. In the time-dependent vehicle networks, each edge's reliability attribute, which is represented by its 95^{th} percentile travel time, is approximated as its average travel time multiplied by a factor of 1.5. Edges traversed by active modes are assumed to have time-invariant travel times such that their reliability attributes equate to their average travel times. Finally, data pertaining to historical scooter locations is generated artificially for 30 days for each time interval by distributing 100 scooters throughout the region in a random uniform way.

For the subsequent examples, the β parameters are defined as $\beta_p = 1$, $\beta_{TT} = \$10$/minute, $\beta_k = \$1$/minute, and $\beta_d = \$0.5$/minute. The value of β_r is adjusted in the fourth case to show how this parameter affects the selection of the least-cost route.

Results

To show the flexibility of the proposed framework, the example for this case study compares the accessibility between the same O-D pair for four separate cases. The first three cases (Case 1, Case 2, and Case 3) use $\beta_r = \$0.75$/minute and the other parameters detailed above. In Case 1, all modes of travel are available, whereas the scooter network is removed in Case 2, and both the scooter and bike share networks are removed in Case 3. The fourth case (Case 4) models the situation where the traveler places a higher value on reliability, indicated by $\beta_r = \$5$/minute, which could be representative of a commuter's mindset en route to work. All modes of travel are permitted in Case 4. To further test the importance of reliability to the commuter, the reliability cost attribute of a public transit boarding edge is increased from $1.5 \cdot TT$ to $2 \cdot TT$. All examples use the same O-D pair, where the origin and destination are the centroids of block groups with FIPS codes 420035623001 and 420031402001, respectively. Comparisons of path costs are made in relative terms since absolute costs do not have physical significance.

The resulting least-cost paths are shown in Figure 5. When all modes are available, the traveler characterized by this set of β parameters has an optimal route that begins the trip with a scooter and finishes with a bike share. The transfer to the bike share network in the middle of the trip can be rationalized by the bike share's cheaper price; the price of a bike share edge is \$0.066 per minute whereas the scooter cost is \$0.39 per minute. This optimal route shows the potential of shared micromobility modes to reduce overall travel costs and improve accessibility for those capable of using active modes of travel.

From Case 1 to Case 2, the generalized travel cost increases by 11.4% as commuters switch from a scooter on the first leg of their trip to public transit. Still, the path includes a bike share for the final segment. The fact that the bike share network is used at the end of the trip in both cases indicates that the destination is in close proximity to a depot, which helps improve the destination's accessibility at least with respect to this particular origin.

In Case 3, the scooter and bike share networks are removed to model the travel preferences of travelers for whom active modes are not a feasible alternative, such as the elderly or disabled.

TABLE 4: Specification of Parameters Used for the Pittsburgh Case Study

Travel Mode	Price	Travel Time	Waiting Time	Risk Index	Discomfort Weight
Personal Vehicle	\$0.64/mile	(speed limit) · (road length)	0 min	$1 + \alpha \cdot$ (crashes/meter)	0
TNC	\$2.55/ride + \$1.75/mile + \$0.35/min	(speed limit) · (road length)	7 min	$1 + \alpha \cdot$ (crashes/meter)	0
Car Share	\$11/60 min	(speed limit) · (road length)	0 min	$1 + \alpha \cdot$ (crashes/meter)	0
Public Transit	\$2.75/ride	GTFS traversal time	(GTFS headway time) / 2	1	0
Personal Bike	\$0.00/ride	(15 km/hr) · (road length)	0 min	1 if bike lane or bike only, else 100,000 if major road, else 1.2	0.30
Bike Share	\$20/300 min	(15 km/hr) · (road length)	0 min	1 if bike lane or bike only, else 100,000 if major road, else 1.2	0.30
Scooter	\$1/ride + \$0.39/min	(15 km/hr) · (road length)	walk time to nearest scooter	1 if bike lane or bike only, else 100000 if major road, else 1.2	0.10
Walk	\$0.00/min	(1.3 m/s) · (road length)	0 min	1	0.10

Note: α is a risk parameter that weights the value of the vehicle crash rate. The parameter $\alpha = 5$ was selected for scaling purposes.

From Case 1 to Case 3, the generalized travel cost increases by 68.6% as these travelers take their full trip using public transit. The least-cost route requires a transfer, which leads to a sizeable increase in travel cost likely due to a waiting penalty. A public transit agency aiming to improve accessibility between this O-D pair specifically for this population group may consider increasing the frequency of the bus line used for the second leg of the trip.

Case 4 results in a route exclusively in the TNC network, even when all other modes are available. Although micromobility modes are reliable in the sense that the 95$^{\text{th}}$ percentile travel time for each edge is equivalent to the edge's average travel time, it still takes longer to commute by active modes as opposed to a private ride share vehicle in the driving network. This means that it could still be the case that the 95$^{\text{th}}$ percentile travel time in a driving network is lower than the average travel time in an active mode network. For a commuter who is highly sensitive to the 95$^{\text{th}}$ percentile travel time between this O-D pair, the TNC network provides an optimal route choice. It is worthwhile to note that the TNC option provides a reliable route due to the assumed reasonable pickup waiting time of 7 minutes. If it were the case that the region had limited TNC drivers and a longer wait time or a high surge price, the optimal path could change.

(a) Case 1: Least-cost route between O-D pair with personal vehicle network excluded.

(b) Case 2: Least-cost route between O-D pair with personal vehicle and scooter networks excluded.

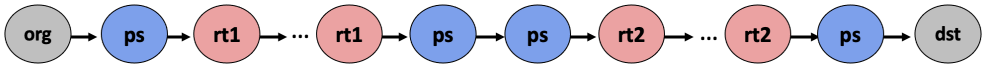

(c) Case 3: Least-cost route between O-D pair with personal vehicle, scooter, and bike share networks excluded.

(d) Case 4: Least-cost route between O-D pair with β_r = \$5/minute and personal vehicle network excluded.

FIGURE 5: Four different least-cost routes are found between the same O-D pair depending on the presence of the micromobility networks and the value of the β_r parameter. "org" = origin, "s" = scooter node, "bs" = bike share depot node, "ps" = physical stop node, "rt" = route node (the number refers, "tnc" = TNC node.

SECTION 2: RELIABILITY ANALYSIS

Once the spatio-temporal probabilistic accessibility of O-D pairs can be quantified between subpopulations and park facilities (as previously outlined), this work proposes a system-level network reliability analysis in which the output is the system-level probability of failure with respect to a given failure limit state (described subsequently), where degradation or insufficient performance of transportation linkages *and/or* the reduction of park facility performance increases the network's probability of failure. This differentiates from existing work in that the performance or quality of the service accessed is considered in both the capacity and demand functions of the reliability analysis; infrastructure management needs to consider the accessibility and *utility* of essential services within the communities they are designed to serve in order to create multi-stakeholder frameworks that can lead to equitable infrastructure design. Another salient example would be consideration of the utility gained by accessing certain grocery stores, which may or may not provide sufficient fresh food options.

From the perspective of city planning officials, the objective is to strategically invest in the park facilities and transportation linkages/assets (e.g., maintenance, rehabilitation, capital projects, addition of micromobility assets) to minimize the system-level probability of failure given cost constraints. Notions of equity are deeply rooted within the proposed network reliability analysis

based on how the failure limit state is defined: a community's system-wide failure is defined as *any* subset of a community's population not being able to access and/or benefit sufficiently from its surrounding community's resources. This ensures that targeted investments are made to reduce a community's network probability of failure subject to the constraint that all subpopulations must remain above a desired accessibility threshold. Because the output of the proposed reward-based reliability method (i.e., probability of failure) is a universal metric that can be directly compared across limit states and capacities and does not vary from location to location, this method provides a way to quantitatively assess and directly compare the health and performance of diverse cities with respect to a single limit state function.

METHODOLOGY

Let $G = (N, A)$ denote the city network graph. The city has C communities and E types of facilities. The types are indexed by e. Then, the set of nodes N contains subsets N_C, N_1, ..., N_E, and N_W, where N_C is the subset of community nodes, N_e is the subset of facility nodes for essential service type e, and N_W is the subset of intermediate nodes. Community node $i \in N_C$ is connected to facility node $j_e \in N_e$ of essential service type e through a series of links. Links $a_\ell \in A$ are indexed by ℓ, and the cardinality of each set is denoted by the operator $|\cdot|$.

For ease of exposition, the following formulation is written for a single essential service type (say, parks), such that the subscript e for the facility node under consideration can be dropped. Assume there are K_{ij} paths connecting community i to facility j, where the value of K_{ij} changes depending on the i,j pair. The optimal path was determined in Section 2. However, we will more broadly present the methodology for the case where this path has not yet been determined a *priori*. Let Q_{ij}^k be an ordered set of connected links that denotes the kth path connecting community i and facility j. If link a_ℓ is on path k connecting i and j, then $a_\ell \in Q_{ij}^k$. Let $\boldsymbol{X}_{ij}$ be the $K_{ij} \times |A|$ link-path incidence matrix whose k-ℓ entry is 1 if $a_\ell \in Q_{ij}^k$ and 0 otherwise. The kth row of the matrix $\boldsymbol{X}_{ij}$ is a Boolean indicator vector that specifies the subset of links present on the kth path between community i and facility j. The $\sum_{i,j} K_{ij} \times |A|$ matrix $\boldsymbol{X}$ is defined as the vertical concatenation of $\boldsymbol{X}_{ij}\ \forall\ i, j$, such that $\boldsymbol{X} = [\boldsymbol{X}_{11}^T | \ldots | \boldsymbol{X}_{1|V|}^T | \boldsymbol{X}_{21}^T | \ldots | \boldsymbol{X}_{2|V|}^T | \ldots | \boldsymbol{X}_{|U|1}^T | \ldots | \boldsymbol{X}_{|U||V|}^T]^T$.

The travel time along each link a_ℓ is characterized by the random variable (RV) T_ℓ. The random vector $\boldsymbol{T} = [T_1, \ldots, T_{|A|}]^T$ is composed of the random link travel times for all links. Let $\boldsymbol{D}$ be a $\sum_{i,j} K_{ij} \times 1$ random vector that contains the path travel times for all possible paths between all i,j pairs. Elements of $\boldsymbol{D}$ are correlated because paths share common links and nearby links can be affected by similar events. Note that $\boldsymbol{D}$ can be divided into constituent vectors $\boldsymbol{D}_{ij}\ \forall\ i,j$, where $\boldsymbol{D}_{ij}$ contains the random path travel times for all paths between community i and facility j, such that $\boldsymbol{D} = [\boldsymbol{D}_{11}^T | \ldots | \boldsymbol{D}_{1|V|}^T | \boldsymbol{D}_{21}^T | \ldots | \boldsymbol{D}_{2|V|}^T | \ldots | \boldsymbol{D}_{|U|1}^T | \ldots | \boldsymbol{D}_{|U||V|}^T]^T$. Since the total travel time along a path is the sum of the travel times along the path's constituent links,

$$\boldsymbol{D} = \boldsymbol{X}\boldsymbol{T} \tag{3}$$

Realizations of the random vectors $\boldsymbol{D}$ and $\boldsymbol{D}_{ij}$ are denoted as $\boldsymbol{d}$ and $\boldsymbol{d}_{ij}$, respectively.

There exists some desired travel time threshold as determined by the managing officials. Let B_{ij} be this travel time limit between community i and facility j, which will herein be referred to as the travel time budget. For simplicity, the travel time budget is assumed to be constant across all i,j pairs. This equity constraint ensures that a fair comparison across communities with respect

Failure Event	Relevant Nodes	Definition
Path k Failure	community u_i and facility v_j	kth element of $\boldsymbol{D}_{ij}$ exceeds C
Accessibility Failure	community u_i and facility v_j	all elements of $\boldsymbol{D}_{ij}$ exceed C
Community Failure	community u_i	attainable utility A_i less than the threshold r_τ
System Failure	all $u_i \in U$	attainable utility A_i less than the threshold r_τ for at least one $u_i \in U$

TABLE 5: Definitions of Failure Events

to their accessibility to a given facility. By this assumption, $B_{ij} = B$.

Each facility j is associated with some utility value, denoted by u_j. Let $\boldsymbol{u} = [u_1, \ldots, u_{|V|}]^T$. If community i can access facility j, then the community can attain the facility's full utility value. The maximum attainable utility value of community i is denoted by A_i. This value can then be compared to the community's desired utility, called u_τ. All $|N_C|$ communities desire the same threshold u_τ, which enables a fair comparison. Each community i desires the same minimum threshold quantity of utility, u_τ.

Failure of path k that connects community i to facility j is defined as the event that the kth element of $\boldsymbol{D}_{ij}$ exceeds B. Failure of community u_i to access facility v_j is defined as the event that all possible paths between the i,j pair fail, which can be written as $\min(\boldsymbol{D}_{ij}) > B$. Failure of community i is defined as the event that the community's maximum attainable utility value, denoted by A_i, is below the threshold u_τ. On a broader scale, failure of the system is defined as the event that any one of the $|N_C|$ communities fails to attain u_τ. A list of failure events and their definitions is presented in Table 5.

Since this problem is principally concerned with the ability of community members to reap the benefits of their public services, such as parks, it is critical to recognize how citizens interact with the facilities corresponding to each type of essential service. For many essential services, community members need only one facility with a utility value that meets their threshold. This case applies to schools and grocery stores; students attend only one school at a time, and people can generally subsist using only one food market that satisfies dietary and cost constraints. On the contrary, access to healthcare and parks is marked by a different dynamic. Across the literature, healthcare access, for example, has been measured in terms of a community's proximity to pharmacies, primary care, dental care, surgical facilities, etc. The use of multiple metrics suggests that just a single facility is insufficient to capture the needs of a community. Thus, two objectives emerge depending on the essential service category: 1) find the probability that a community accesses at least one facility that meets their utility threshold, and 2) find the probability that a community can access multiple facilities whose total utility meets their threshold. For park facilities, we explore the later of these two cases.

Reliability Analysis

Let $\boldsymbol{Y}$ be a $|U| \times |V|$ random binary matrix whose i-j entry is 1 if community u_i accesses facility v_j, and 0 otherwise. Since each element of the matrix $\boldsymbol{Y}$ can be either 0 or 1, there are $2^{|U|*|V|}$ possible

realizations of $\boldsymbol{Y}$. The full set of realizations, which is indexed by s, composes the domain of $\boldsymbol{Y}$. The domain of $\boldsymbol{Y}$ is then given by $S(\boldsymbol{Y}) = \{\boldsymbol{y}_s, s = 1,2,\ldots,2^{|U|*|V|}\}$, where $\boldsymbol{y}_s$ is a single realization of $\boldsymbol{Y}$.

Recall that a community u_i is said to be able to successfully access facility v_j if at least one path between the pair has a path travel time realization below or equivalent to the travel time budget C. The probability that the accessibility success event occurs for the i,j pair can be found as $\mathrm{P}(\min(\boldsymbol{D}_{ij}) \leq C)$. Conversely, the accessibility failure event for community u_i facility v_j occurs if all paths have travel time realizations above C. The probability that the failure event occurs for the i,j pair can be found as $\mathrm{P}(\min(\boldsymbol{D}_{ij}) > C)$.

Each realization $\boldsymbol{y}_s$ of the $|U| \times |V|$ random binary matrix $\boldsymbol{Y}$ represents a different combination of joint accessibility success and failure events across all i,j pairs. Accessibility success and failure events are dependent because elements of $\boldsymbol{D}$ are correlated. Define the accessibility set $\mathscr{A}_s$ as the ordered pairs of communities and facilities for which the accessibility success event occurred in realization $\boldsymbol{y}_s$; these are the i,j pairs corresponding to the elements of $\boldsymbol{y}_s$ whose values are 1. Define the complementary failure set $\mathscr{A}_s^C$ as the ordered pairs of communities and facilities for which the accessibility failure event occurred in realization $\boldsymbol{y}_s$; these are the i,j pairs corresponding to the elements of $\boldsymbol{y}_s$ whose values are 0. The probability of each realization $\boldsymbol{y}_s$ is then the joint probability of the accessibility success and failure events that compose it:

$$P(\boldsymbol{y}_s) = P\left(\bigcap_{(i,j)\in\mathscr{A}_s} \min(\boldsymbol{D}_{ij}) \leq C \cap \bigcap_{(i,j)\in\mathscr{A}_s^C} \min(\boldsymbol{D}_{ij}) > C\right) \tag{4}$$

Now consider the random variable A_i, which represents the total utility attained by community u_i. Let $\boldsymbol{A} = [A_1, A_2, \ldots, A_{|U|}]^T$, such that $\boldsymbol{A}$ is a $|U| \times 1$ discrete random vector representing the joint distribution of total attained utility for each of the $|U|$ communities. It is important to note that the components of $\boldsymbol{A}$ are correlated since accessibility success and failure events are dependent. The vector $\boldsymbol{A}$ has $2^{|U|*|V|}$ possible realizations, also indexed by s. Note that the realization $\boldsymbol{y}_s$ and $\boldsymbol{a}_s$ share the common index s because they are defined by the same unique combination of accessibility success and failure events. Recall that $\boldsymbol{r}$ is the deterministic utility vector whose jth element is the utility value associated with facility j. Since a community receives a facility's full utility only when accessing it, the domain of $\boldsymbol{A}$ is given by, $S(\boldsymbol{A}) = \{\boldsymbol{a}_s = \boldsymbol{y}_s\boldsymbol{r}, s = 1,2,\ldots,2^{|U|*|V|}\}$.

The probability of each realization $\boldsymbol{a}_s$ is then equivalent to the probability of $\boldsymbol{y}_s$, which can be found by Equation 4. Once the joint probability mass function (PMF) of $\boldsymbol{A}$ has been enumerated explicitly in this manner, the marginal PMF of A_i can be determined for all $u_i \in U$. The probability of failure of a single community u_i, denoted by $P_{F,i}$, can then be found simply as,

$$P_{F,i} = F_{A_i}(r_{thresh}) \tag{5}$$

where $F_{A_i}(\cdot)$ denotes the cumulative distribution function (CDF) of A_i. This calculation completes the first objective. Furthermore, the probability of system failure, $P_{F,sys}$ is defined as the probability that at least one community fails. $P_{F,sys}$ is equivalent to the probability of the union of all community failure events, given by,

FIGURE 6: Community need scores, site need scores, and environmental overlay scores are used to inform the Pittsburgh Parks Conservancy's final Investment Priority Score for (*6*).

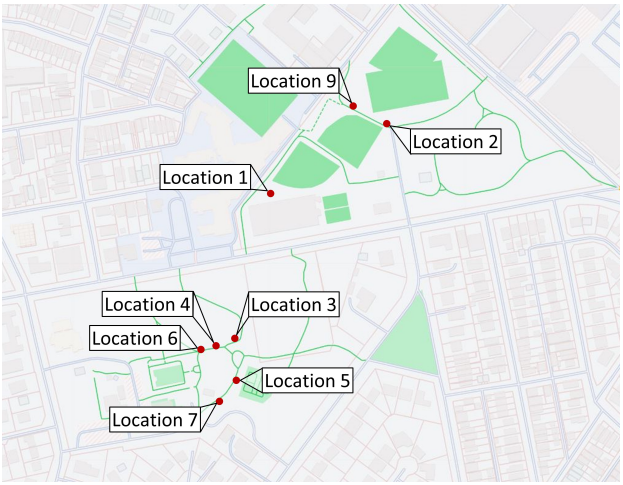

FIGURE 7: Sensing node deployment locations across the top (north of 5th Avenue) and bottom (south of 5th Avenue) halves of Mellon Park.

$$P_{F,sys} = P\left(\bigcup_{i=1}^{|U|}(A_i < r_{thresh})\right) \tag{6}$$

This calculation completes the evaluation of the system-level probability of failure.

SECTION 3: MEASURING THE PERFORMANCE OF PARK FACILITIES

The third part of this research seeks to incorporate real-time metrics into the Park Scoring database to assess the need for asset improvements. The Park Scoring Database comprises the first-ever comprehensive inventory of all park and recreation sites, assessment information on park needs, community needs, and public priorities, as well as extensive demographic, health, community condition, and ecological information. Community input was collected over the course of 240 listening tours that were conducted across 70 Pittsburgh neighbor-hoods. In addition to feedback collected during the tours, 3,400 surveys were administered to determine public priorities for park investment. However, these metrics (shown in Figure 6) lack real-time metrics quantifying usage, human-human sociability, or human-asset interaction. To highlight the importance of integrating

(a) (b) (c)

FIGURE 8: Examples of three of the eight sensing nodes installed at (a) Location 1, (b) Location 3, and (c) location 6.

real-time monitoring based on in situ measurements into the park scores, the PI will reflect on a previous experience. During the late summer and fall of 2018, the PI used a network of *Urbano* sensing nodes to monitor pedestrian traffic on a section of a vital pathway connecting an under-resourced community to the Detroit Riverfront (Detroit, MI). Pedestrian use data was collected in real time and several use trends and correlations were observed including correlations between weather and trail usage as well as the numbers of pedestrians at various times of the day. A series of unexplained periods of drastically reduced trail usage were also regularly observed. After visiting and investigating the location it was determined that these periods of little to no pedestrian traffic were correlated to unexpected (i.e., not anticipated by the urban planners) severe flooding along the trail due to the storm sewer inlet infrastructure not functioning properly; this critical pathway was rendered unusable for several days following any rain event.

Park usage and associated health/performance metrics are measured directly using a low-power wireless sensing archicture developed by the PI. Each sensing node, called *Urbano* (from the Latin urbanus, "of or belonging to a city", derived from urbs, "city"), is an Internet of Tings-(IOT) based technology that supports interoperability among diverse arrays of heterogeneous IoT devices, preserves privacy and trust among citizens, supports cloud-based analytics, and has a user-friend design. For example, discrete pedestrian counts (measured from passive infrared, or "PIR", sensors) are collected from distributed sensing nodes. Because *Urbano* nodes support low-power and low-cost sensing and use cellular communication to free nodes from fixed power sources (relying instead on small solar panels for solar harvesting), they can be deployed in under-resourced areas, enabling decision makers to make data-driven investments in neighborhoods that have historically been underserved. This addresses the urgent need for quantitative approaches to integrated park and transportation design and management in under-resourced areas to ensure that investments made in parks using limited tax dollars have maximum effect. In situ data measured using *Urbano* nodes is transmitted to a cloud-based server and provides a wealth of information that will be used to characterize usage subject to, for example, daily environmental (i.e., weather) and operational conditions. This can also be used to capture "before" and "after" data to quantify the impact

of asset and infrastructure management decisions made by the City of Pittsburgh and Pittsburgh Parks Conservancy.

FIGURE 9: Lawn signs inform park users about the scope of the project and data collected.

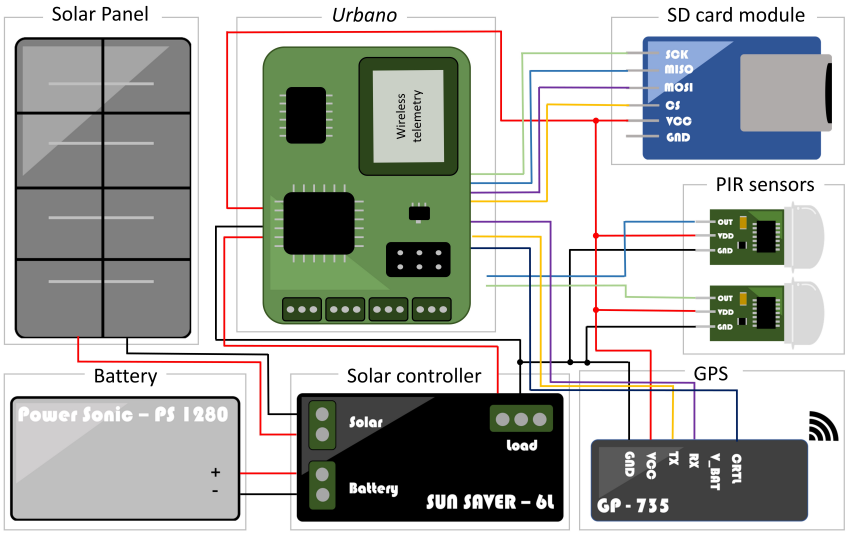

FIGURE 10: Sensing node circuit configuration.

For this project, a network of eight sensing nodes (Figure 7) were installed across Mellon Park in Pittsburgh, PA. The only limitation of the size of the network was the availability of light poles (which are used for the installation to keep the sensing nodes out of reach). As requested by the City of Pittsburgh, each sensing node is accompanied by a lawn sign (Figure 9) that provides information about the project, states the objective of the data collection, and lets users know that the data is full privacy preserving.

A schematic of the *Urbano* nodes designed, built, and deployed for this project is shown in Figure 9. A 12V rechargeable lead acid batter, solar controller, two PIR sensors, GPS module,

Urbano node, and SD card module are packaged within a water-tight enclosure and connected to an external 10-watt solar panel. A hard copy of all data is backed up on the external SD card. Time-synchronization is achieved across sensing units using GPS. Pedestrians and bikers are counted immediately when they pass along the paths in front of the nodes. When users move from left to right in front of the node, data is collected as: ``06/08/202209:00:15-RIGHT''. When users move from right to left in front of the node, data is collected as: ``06/08/202208:56:02-LEFT''. Due to installation delays caused by the COVID-19 pandemic (which resulted in the installation not being signed off by the administration until mid-Summer 2022), the team is in the early stages of data collection. The team anticipates working with park managers (after several months of data are collected) to start co-creating a usage performance metric that will integrate into their scoring database based on the real-time data.

CONCLUSION

The research described in detail in this report explores urban park use and correlates of use (measured by time-dependent accessibility) in order to bring to light ways in which city officials and planners can quantify data-driven returns on potential investments to parks and mobility services and implement changes that will more equitably distribute these benefits. This report presents the problem descriptions, approaches, methodologies, and findings for three primary thrust required to achieve the overarching project goal: 1) development of a novel multimodal network modeling framework that accounts for five major factors across all travel modes: day-to-day average travel time, price, reliability represented by day-to-day travel time variability, safety risks, and discomfort (i.e., quantify community accessibility to parks across time and space), 2) quantification of the total system performance through a probabilistic spatio-temporal network reliability analysis in which the failure limit state is defined as any subset of a community's population not being able to access and/or benefit sufficiently from its surrounding parks (note that this is a function of both park performance and accessibility), and 3) integration of privacy-preserving cyber-physical system technologies that measure park usage into Pittsburgh parks (i.e., quantitatively measure and integrate the performance of parks into the Park Scoring Database)

The modeling framework developed in this project successfully evaluates time dependent accessibility in a multimodal network. This framework builds upon previous literature in several ways. First, it incorporates all relevant mobility options including personal vehicle, TNC, car share, public transit, personal bike, bike share, scooter, and walking. In addition, it defines a generalized travel cost function that accounts for average travel time, price, reliability, risk, and discomfort, as well as a movement-based node cost that can impose additional (dis)incentives for any multimodal trip. Since each factor is assigned a weight that represents its value to the traveler, these weights can be tailored to different population groups. This framework can be used by transportation planners as they evaluate where to add and improve mobility services and mobility infrastructure with the goal of creating a more accessible and equitable mobility system. Planners can also use this model to examine how any change to mobility services can potentially impact individual travelers with different starting points, departure times, or socio-demographics.

To demonstrate this model in real-world large-scale network, four scenarios are explored in the Pittsburgh metropolitan network. The results exhibit the potential of micromobility to improve access between a specific O-D pair by leading to a sizable reduction in generalized travel cost relative to the baseline public transit and walking case. The case study also highlights the ability to account for different population groups via parameter adjustment, which points to an opportunity

for future work in sensitivity analysis of the various parameters and cost functions. The PI recommends that continuation of this work should involve estimation of the pattern of network usage for each mode and facility in high granularity. This can be accomplished by aggregating least-cost paths for all individuals across multiple O-D pairs to find commonly-used nodes and links. Such an assessment could inform a decision on when, where, and how to improve mobility services.

Once the spatio-temporal probabilistic accessibility of O-D pairs is quantified between subpopulations and park facilities (as stated previously), this work proposes a system-level network reliability analysis in which the output is the system-level probability of failure with respect to a given failure limit state. By defining the failure limit state to be any subset of a community's population not being able to access and/or benefit sufficiently from its surrounding community's park facilities, the research team finds that system-level performance can be effectively characterized by degradation or insufficient performance of the transportation linkages *and/or* the reduction of park facility performance. This radically differentiates itself from existing work in that the performance or quality of the service accessed is considered in both the capacity and demand functions of the reliability analysis; management of infrastructure (in this case parks) needs to consider the accessibility and utility of essential services within the communities they are designed to serve in order to better create multi-stakeholder frameworks that can lead to equitable infrastructure design.

For this project, the aforementioned performance of park assets is measured by the Park Scoring database. This project delivers the design, construction, and installation of a wireless sensing network used to monitor pedestrian and bike traffic in Pittsburgh's Mellon Park. Due to installation delays caused by the COVID-19 pandemic (which resulted in the installation not being signed off by the administration until mid-Summer 2022), the team is in the early stages of data collection. Next steps will include taking collected data and incorporating real-time metrics into the Park Scoring database that account for park usage.

Looking forward, there are three key research thrust developed in this work that will be further leveraged: spatio-temporal multimodal accessibility, system-level reliability that accouts for accessibility and park facility performance, and quantification of park facility performance using cyber-physical system technologies. For the purpose of making optimal urban planning and investment decisions, the research team plans to continue the existing stakeholder partnerships to simulate the effects of specific park and mobility service maintenance, rehabilitation, and capital projects on park facility accessibility. This will enable decision makers to understand which mobility options have the potential to improve accessibility, gain insights into spatio-temporal mobility disparities across different populations with different needs, and incorporate real-time metrics into the Park Score database to assess the need for asset improvements.

REFERENCES

1. Neema, M. N. and A. Ohgai, Multi-objective location modeling of urban parks and open spaces: continuous optimization. *Computers, Environment and Urban Systems*, Vol. 34, 2021, pp. 359–376.
2. Pittsburgh Parks Conservancy, *Benefits of Pittsburgh's Parks System*, 2019, https://pittsburghparks.org/wp-content/uploads/2020/10/PPC_RPP_Benefits_Case_0911-4.pdf, Last accessed on 2020-12-10.
3. The Trust for Public Land, *Pittsburgh, PA ParkScore Ranking*, 2019, https://www.tpl.org/city/pittsburgh-pennsylvania, Last accessed on 2020-12-10.
4. The Trust for Public Land, *Parks Listening Tour Phase II*, 2020, https://pittsburghparks.org/wp-content/uploads/2020/10/PPC-Parks-For-All-Presentation-V7-2.pdf, Last accessed on 2020-04-15.
5. Pittsburgh Parks Conservancy, *Restoring Pittsburgh Parks*, 2020, https://pittsburghparks.org/our-work/restoring-pittsburgh-parks/, Last accessed on 2020-04-15.
6. Pittsburgh Parks Conservancy, *Park Scoring Database*, 2020, https://pittsburghparks.org/wp-content/uploads/2020/10/Park-Ranking-Sheet-2019-07-31.pdf, Last accessed on 2020-04-15.
7. Jones, K. and A. Kirby, Provision and wellbeing: an agenda for public resources research. *Environment and Planning A: Economy and Space*, Vol. 14, 1982, pp. 297–310.
8. Kirby, A., P. Knox, and S. Pinch, Developments in public provision and urban politics: an overview and agenda. *Area*, Vol. 15, 1983, pp. 295–300.
9. Pinch, S., Inequality in pre-school provision: a geographical perspective. In *Public service provision and urban development* (A. Kirby, P. Knowx, and S. Pinch, eds.), Croom Helm, London, 1984, pp. 231–282.
10. Smith, D., *Geography and social justice*. Blackwell, Oxford, 1994.
11. Hay, A., Concepts of equity, fairness and justice in geographical studies. *Transactions of the Institute of British Geographer*, Vol. 20, 1995, pp. 500–508.
12. Talen, E. and L. Anselin, Assessing spatial equity: an evaluation of measures of accessibility to public playgrounds. *Environment and Planning*, Vol. 30, 1998, pp. 595–613.
13. Ogryczak, W., Inequality measures and equitable approach to location problems. *European Journal of Operational Research*, Vol. 122, 2000, pp. 374–391.
14. *Austin Strategic Mobility Plan*, 2022, https://www.austintexas.gov/sites/default/files/files/Transportation/ASMP/AdoptedASMP_Executive_Summary_and_Introduction2022.pdf, Last accessed on 2022-08-01.
15. *Go Boston 2030*, 2017, https://www.boston.gov/departments/transportation/go-boston-2030#report-chapters, Last accessed on 2022-08-01.
16. *Portland's 2035 Transportation System Plan*, 2022, https://www.portland.gov/sites/default/files/2020-05/tsp-101-two-pager-03-21-2019_0.pdf, Last accessed on 2022-08-01.
17. Tribby, C. P. and P. A. Zandbergen, High-resolution spatio-temporal modeling of public transit accessibility. *Applied Geography*, Vol. 34, 2012, pp. 345–355.

18. Djurhuus, S., H. Sten Hansen, M. Aadahl, and C. Glümer, Building a multimodal network and determining individual accessibility by public transportation. *Environment and Planning B: Planning and Design*, Vol. 43, No. 1, 2016, pp. 210–227, publisher: SAGE Publications Ltd STM.
19. El-Geneidy, A., D. Levinson, E. Diab, G. Boisjoly, D. Verbich, and C. Loong, The cost of equity: Assessing transit accessibility and social disparity using total travel cost. *Transportation Research Part A: Policy and Practice*, Vol. 91, 2016, pp. 302–316.
20. Chen, J., J. Ni, C. Xi, S. Li, and J. Wang, Determining intra-urban spatial accessibility disparities in multimodal public transport networks. *Journal of Transport Geography*, Vol. 65, 2017, pp. 123–133.
21. Järv, O., H. Tenkanen, M. Salonen, R. Ahas, and T. Toivonen, Dynamic cities: Location-based accessibility modelling as a function of time. *Applied Geography*, Vol. 95, 2018, pp. 101–110.
22. Carpentieri, G., C. Guida, and H. E. Masoumi, Multimodal Accessibility to Primary Health Services for the Elderly: A Case Study of Naples, Italy. *Sustainability*, Vol. 12, No. 3, 2020, p. 781, number: 3 Publisher: Multidisciplinary Digital Publishing Institute.
23. Yu, W., H. Sun, T. Feng, J. Wu, Y. Lv, and G. Xin, A Data-Based Bi-Objective Approach to Explore the Accessibility of Multimodal Public Transport Networks. *ISPRS International Journal of Geo-Information*, Vol. 10, No. 11, 2021, p. 758, number: 11 Publisher: Multidisciplinary Digital Publishing Institute.
24. Curtis, C. and J. Scheurer, Planning for sustainable accessibility: Developing tools to aid discussion and decision-making. *Progress in Planning*, Vol. 74, No. 2, 2010, pp. 53–106.
25. Dimokas, N., K. Kalogirou, P. Spanidis, and D. Kehagias, A Mobile Application for Multimodal Trip Planning. In *2018 9th International Conference on Information, Intelligence, Systems and Applications (IISA)*, 2018, pp. 1–8.
26. Delling, D., T. Pajor, and D. Wagner, Accelerating Multi-modal Route Planning by Access-Nodes. In *Algorithms - ESA 2009* (A. Fiat and P. Sanders, eds.), Springer, Berlin, Heidelberg, 2009, Lecture Notes in Computer Science, pp. 587–598.
27. Zhang, J., F. Liao, T. Arentze, and H. Timmermans, A multimodal transport network model for advanced traveler information systems. *Procedia - Social and Behavioral Sciences*, Vol. 20, 2011, pp. 313–322.
28. Delling, D., J. Dibbelt, T. Pajor, D. Wagner, and R. F. Werneck, Computing Multimodal Journeys in Practice. In *Experimental Algorithms* (V. Bonifaci, C. Demetrescu, and A. Marchetti-Spaccamela, eds.), Springer, Berlin, Heidelberg, 2013, Lecture Notes in Computer Science, pp. 260–271.
29. Hrnčíř, J. and M. Jakob, Generalised time-dependent graphs for fully multimodal journey planning. In *16th International IEEE Conference on Intelligent Transportation Systems (ITSC 2013)*, 2013, pp. 2138–2145, iSSN: 2153-0017.
30. Dibbelt, J., T. Pajor, and D. Wagner, User-Constrained Multimodal Route Planning. *ACM Journal of Experimental Algorithmics*, Vol. 19, 2015, pp. 1–19.
31. Georgakis, P., A. Almohammad, E. Bothos, B. Magoutas, K. Arnaoutaki, and G. Mentzas, MultiModal Route Planning in Mobility as a Service. In *IEEE/WIC/ACM International Conference on Web Intelligence - Companion Volume*, ACM, Thessaloniki Greece, 2019, pp. 283–291.

32. Huang, H., D. Bucher, J. Kissling, R. Weibel, and M. Raubal, Multimodal Route Planning With Public Transport and Carpooling. *IEEE Transactions on Intelligent Transportation Systems*, Vol. 20, No. 9, 2019, pp. 3513–3525, conference Name: IEEE Transactions on Intelligent Transportation Systems.
33. Carlier, K., T. Inro, S. Fiorenzo-catalano, C. Lindveld, P. Bovy, K. Carlier, S. Fiorenzo-catalano, C. Lindveld, and P. Bovy, A supernetwork approach towards multimodal travel modeling. In *Proceedings of the 81st Transportation Research Board Annual Meeting, Washington DC*, 2003.
34. Liao, F., T. Arentze, and H. Timmermans, Supernetwork Approach for Multimodal and Multiactivity Travel Planning. *Transportation Research Record*, Vol. 2175, No. 1, 2010, pp. 38–46, publisher: SAGE Publications Inc.
35. Ni, P., H. T. Vo, D. Dahlmeier, W. Cai, J. Ivanchev, and H. Aydt, DEPART: Dynamic Route Planning in Stochastic Time-Dependent Public Transit Networks. In *2015 IEEE 18th International Conference on Intelligent Transportation Systems*, 2015, pp. 1672–1677, iSSN: 2153-0017.
36. Boeing, G., OSMnx: New methods for acquiring, constructing, analyzing, and visualizing complex street networks. *Computers, Environment and Urban Systems*, Vol. 65, 2017, pp. 126–139.
37. Liu, L., Data Model and Algorithms for Multimodal Route Planning with Transportation Networks (Doctoral dissertation), 2010.
38. Abdel-Aty, M., J. Lee, C. Siddiqui, and K. Choi, Geographical unit based analysis in the context of transportation safety planning. *Transportation Research Part A: Policy and Practice*, Vol. 49, 2013, pp. 62–75.
39. Pu, W., Analytic Relationships between Travel Time Reliability Measures. *Transportation Research Record*, Vol. 2254, No. 1, 2011, pp. 122–130, publisher: SAGE Publications Inc.
40. Center, A. F. D., *Active Transportation and Micromobility*, ????, `https://afdc.energy.gov/conserve/active_transportation.html`, Last accessed on 2022-08-01.
41. Chabini, I., Discrete Dynamic Shortest Path Problems in Transportation Applications: Complexity and Algorithms with Optimal Run Time. *Transportation Research Record*, Vol. 1645, No. 1, 1998, pp. 170–175, publisher: SAGE Publications Inc.
42. Zou, Q., S. Qian, S. Detweiler, and R. Chajer, Estimating Dynamic Origin-Destination Demand for Multi-modal Transportation Networks: A Computational Graph-Based Approach (Working Paper), 2022.
43. Western Pennsylvania Regional Data Center, 2022, `http://www.wprdc.org/`, Last accessed on 2022-08-01.
44. Zipcar, 2022, `https://www.zipcar.com/pittsburgh`.
45. Maps, G. M., 2022, `https://www.google.com/maps/d/u/0/`.
46. POGOH, 2022, `https://pogoh.com/`.
47. SPIN, 2022, `https://www.spin.app/`, Last accessed on 2022-08-01.
48. Transit, P. R., 2022, `https://www.portauthority.org/`.
49. Hughes, R. and D. MacKenzie, Transportation network company wait times in Greater Seattle, and relationship to socioeconomic indicators. *Journal of Transport Geography*, Vol. 56, 2016, pp. 36–44.

50. Orendurff, M. S., G. C. Bernatz, J. A. Schoen, and G. K. Klute, Kinetic mechanisms to alter walking speed. *Gait & Posture*, Vol. 27, No. 4, 2008, pp. 603–610.
51. Schleinitz, K., T. Petzoldt, L. Franke-Bartholdt, J. Krems, and T. Gehlert, The German Naturalistic Cycling Study – Comparing cycling speed of riders of different e-bikes and conventional bicycles. *Safety Science*, Vol. 92, 2017, pp. 290–297.
52. Liu, M., E. Brynjolfsson, and J. Dowlatabadi, Do Digital Platforms Reduce Moral Hazard? The Case of Uber and Taxis. *Management Science*, Vol. 67, No. 8, 2021, pp. 4665–4685, publisher: INFORMS.
53. AAA, *Your Driving Costs: 2021*, 2021, https://newsroom.aaa.com/wp-content/uploads/2021/08/2021-YDC-Brochure-Live.pdf.
54. Ansari Esfeh, M., S. C. Wirasinghe, S. Saidi, and L. Kattan, Waiting time and headway modelling for urban transit systems – a critical review and proposed approach. *Transport Reviews*, Vol. 41, No. 2, 2021, pp. 141–163.